ISBN: 978-3-95450-215-8 ISSN: 2226-0366 doi:10.18429/JACoW-LINAC2022-TUPOJO06

DESIGN AND TEST OF BEAM DIAGNOSTICS EQUIPMENT FOR THE FAIR PROTON LINAC

T. Sieber†, P. Forck, C. Kleffner, S. Udrea, GSI, Darmstadt, Germany
J. Herranz, PROACTIVE R&D, Sabadell, Spain
I. Bustinduy, A. Rodriguez Paramo, ESS Bilbao, Zamudio, Spain
A. Navarro Fernandez, CERN, Geneva, Switzerland

Abstract

A dedicated proton injector Linac (pLinac) for the Facility of Antiproton and Ion Research (FAIR) at GSI, Darmstadt, is currently under construction. It will provide a 68 MeV, up to 70 mA proton beam at a duty cycle of max. 35µs / 2.7 Hz for the SIS18/SIS100 synchrotrons, using the existing UNILAC transfer beamline. After further acceleration in SIS100, the protons are mainly used for antiproton production at the Pbar ANnihilations at DArmstadt (PANDA) experiment. The Linac will operate at 325 MHz and consists of a novel so called 'Ladder' RFQ type, followed by a chain of CH-cavities, partially coupled by rf-coupling cells. In this paper we present the beam diagnostics system for the pLinac with special emphasis on the Secondary Electron Emission (SEM) Grids and the Beam Position Monitor (BPM) system. We also describe design and status of our diagnostics testbench for stepwise Linac commissioning, which includes an energy spectrometer with associated optical system. The BPMs and SEM grids have been tested with proton and argon beam during several beamtimes in 2022. The results of these experiments are presented and discussed.

INTRODUCTION

The FAIR [1] facility at GSI will provide antiproton and ion beams of worldwide unique intensity and quality for fundamental physics research.

The accelerator facility of FAIR, shown in Fig. 1, will include three linear accelerators, the existing UNILAC (for which a refurbishing program is currently on the way), a superconducting cw-Linac, designed mainly for intermediate energy experiments [2], and the new proton Linac [3] (pLinac). The UNILAC and pLinac will be the main injectors of SIS18, which will in turn be an injector for SIS100, the central accelerator component of FAIR.

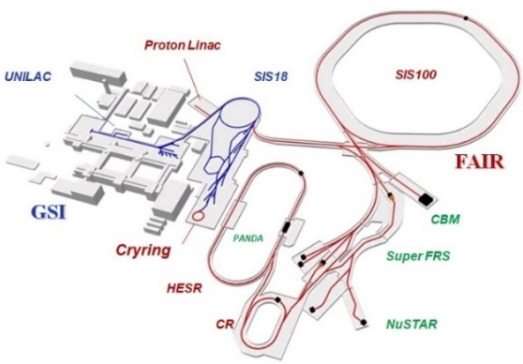

Figure 1: Layout of the FAIR facility.

†T.Sieber@gsi.de

The pLinac consists of a novel so called 'Ladder' RFQ [4] followed by two ~10 m sections of Cross Bar H-drift-tube accelerator (CH) structures [5]. The first section includes six CH modules, which are pairwise rf-coupled (Coupled CH or CCH). The second section consists of three separate modules, each connected to its own klystron. The pLinac will deliver a current up to 70 mA with a macropulse length of 35 µs (at max. 4 Hz) and a typical bunch length of 100 ps. The design energy is 68 MeV. Figure 2 shows a schematic of the pLinac and its beam instrumentation.

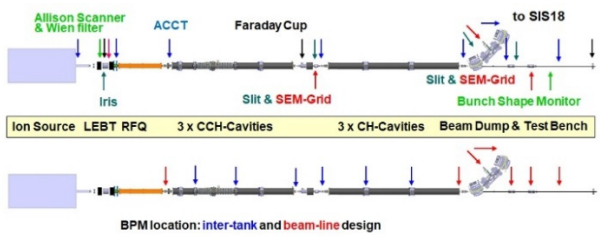

Figure 2: Schematic of the FAIR pLinac, side view, showing the location of diagnostics (upper) and BPMs, divided in cavity (inter-tank) and beamline BPMs (lower).

The overall diagnostics concept and layout of pLinac has been described in various reports, e.g. [6]. Because of the compact structure of the two CH sections, diagnostics (except BPMs) will be concentrated in the LEBT, in the MEBT behind the RFQ and in a diagnostics/rebuncher (so called SD) section between the CCH and CH parts of the pLinac. Additional beam diagnostics elements are placed in the transfer line to SIS18 as well as in a straight line to the beam dump.

Concerning the SEM Grid design (Fig. 3), we expect a 1σ beam radius of 1.5 mm at best possible beam quality in pLinac, therefore the wire pitch cannot be larger than 0.5 mm to obtain reasonable profiles. To compensate for thermal expansion of the wires, a stretching mechanism is required - even if the grids are operated in a 'grid protection mode' at reduced duty cycle. Gold plating on the tungsten wires has to be considered carefully because of possible melting and agglutination during irradiation.

The BPM system of pLinac [7] comprises button BPMs, as shown in Fig. 4, in combination with a custom made preamplifier including narrowband amplification (single button signals) for the frequency domain LIBERA (Single Pass H, LSPH) electronics and wideband amplification (sum signal) for oscilloscope based time of flight (TOF) measurements.

ISBN: 978-3-95450-215-8 ISSN: 2226-0366 doi:10.18429/JACoW-LINAC2022-TUPOJO06

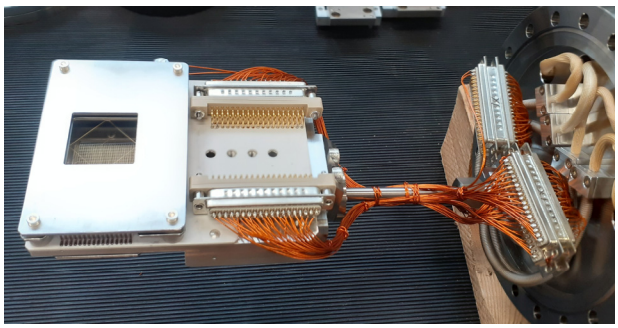

Figure 3: SEM harp by PROACTIVE. The grid consists of two harps rotated by 90°, area 32 mm x 32 mm with diamond shaped cleaning electrode, 64 wires per harp, wire pitch 0.5 mm, thickness 100 µm.

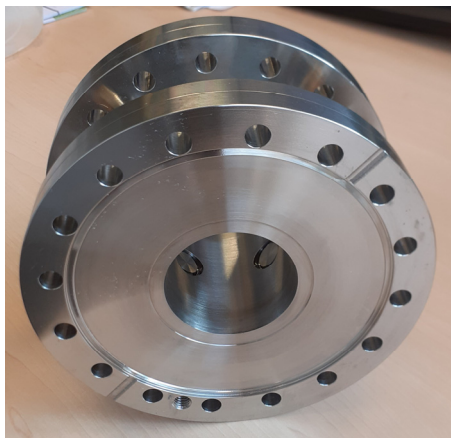

Figure 4: Beamline BPM by NTG. Aperture 50 mm, button diameter 12 mm, total length 80 mm, DN100CF.

Our testbench for stepwise Linac commissioning, which is currently under construction, will be described in the last section.

SEM GRID ACCEPTANCE TEST

The test of two prototype y-harps (gold coated / uncoated tungsten wires) was performed in two steps, in a first campaign a low intensity proton beam was used to prove the correct function of the harp in connection with the POLAND+CSA electronics [8] (proton beam parameters, see BPM section). A second experimental campaign was performed with a high intensity Ar beam to check the wire stretching system, the upper limit of acceptable energy deposition and the actual heat load in comparison to simulations. The beamtime started with gold-plated wires, later we switched to a harp with regular tungsten wires. We used an Ar^{10+} beam at 8.6 MeV/u, intensities 20 µA to 1.5 mA, pulse length 40 µs to 200 µs, repetition rate 1 Hz. In parallel to the measurements, simulations for wire heating were done with the pyTT code [9], predicting the wire temperature at the various measurements.

We checked the effect of the voltage on the diamond shaped cleaning electrode (extraction of secondary electrons to reduce wire cross-talk) while varying beam parameters. Figure 5 shows the voltage dependence of the integrated number of particles for two different spot sizes.

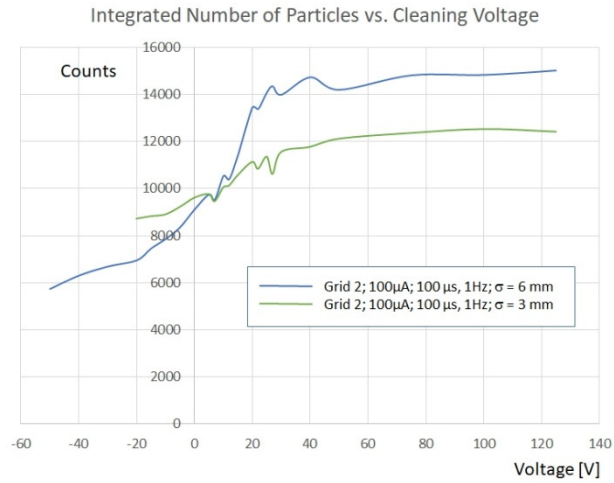

Figure 5: Number of particles, as a function of cleaning voltage. Sigma values indicate the beam size assuming gaussian distribution in the calculations.

If the maximum current on the grid wires (maximum total counts) is taken as a criterion for optimum voltage, there is obviously not much effect from the cleaning electrode above ~40 V, which significantly reduces the effort for electrical connections. With proton beam, the saturation voltage was even smaller (<10 V). A comparison of the two curves in Fig. 5 shows that the number of counts is reduced most likely due to geometrical aspects at the smaller number of wires, while an effect on the slope of the curves cannot be observed (at given accuracy), which is a strong hint for a homogeneous field distribution as result of our electrode geometry optimization.

At inspection the gold plated grid showed no damage, even after heating to (theoretically) >2500 K. From this we concluded, that the wire temperature might have been overestimated in our calculations. Beam parameters (such as beam size, beam intensity, pulse length, etc.) and material properties (such as emissivity) are crucial for accurate thermal modeling. Big uncertainties on beam spot size and the emissivity of the material yielded too large uncertainties in the predicted temperatures. In an ideal case, temperature calibration measurements should be performed, which could not be done for several reasons. Thus, a systematic approach has been adopted to prove the suitability of the SEM grids. The harp was irradiated in the regular UNILAC 'grid protection mode', which at a spot size of σ = 3 mm an intensity of 500 µA and duration of 40 µs corresponds to a (calculated) temperature of ~2800 K. Starting from this point, the intensity and the pulse length were stepwise increased to 1.4 mA, 40 µs, which lead after a final step to 70 µs to destruction of some wires (T_{calc} = ~4200 K). The reasons for the strong increase of the current in Fig. 6, besides the position of the broken wires, and it's duration is to be discussed. Several aspects contribute to the dynamic development of the profile, like time constant of the electronics and intensity variation during macro pulse.

ISBN: 978-3-95450-215-8 ISSN: 2226-0366 doi:10.18429/JACoW-LINAC2022-TUPOJO06

To what extent thermionic emission plays a role has to be investigated. Analysis of the results and adjustment of our theoretical model is ongoing.

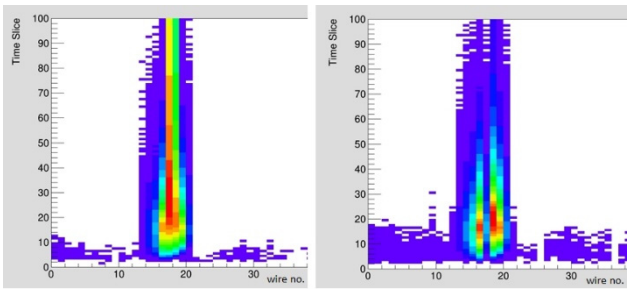

Figure 6: Development of the beam profile during a 70 µs macro pulse before (left) and after (right) destruction of one wire. A time slice corresponds to 5 µs.

TEST OF THE BPM SYSTEM

A proton beamtime at UNILAC had the purpose to test the whole BPM chain for the first time: button BPMs, preamplifier, LIBERA electronics as well as the FESA control software. We used an 8.6 MeV proton beam with an intensity of 100 - 300 µA and two BPMs, as shown in Fig. 4, installed 325.5 mm apart from each other to allow for TOF measurements. The bunches arrived with 36 MHz, the high current injector operation frequency, we used a 50 µs window within the 200 µs macro pulse (1 Hz operation).

During the tests, the full functionality of the system could be demonstrated. Position and TOF measurements with the LSPH/FESA were verified by parallel oscilloscope measurements. The various algorithms in FESA, for position [10] and phase calculation, showed excellent agreement. By variation of the beam current it was shown that the FESA class switches dynamic range as required. In total the system is - except for minor optimization steps and a missing GUI - considered ready for operation. An interesting side aspect of the tests was that dispersive effects in the beam transport at UNILAC could be identified by phase (and also position) shift between the horizontal buttons. Fig. 7 shows data read out directly from the LSPH. The x-position measurement shown in the middle nicely illustrates how the beam position changes during the macro pulse, induced by the bending dipoles. The phase measurement shows accordingly how the left side of the beam (orange) precedes the right side (red).

DIAGNOSTICS TESTBENCH

Since the pLinac consists entirely of novel accelerating structures, a detailed step-by-step characterization of each cavity is essential. The testbench for stepwise commissioning shown in Fig. 8 will consist of all relevant types of diagnostic devices that have been developed for the pLinac and additionally a magnetic spectrometer for measurements of the proton beam's energy spread.

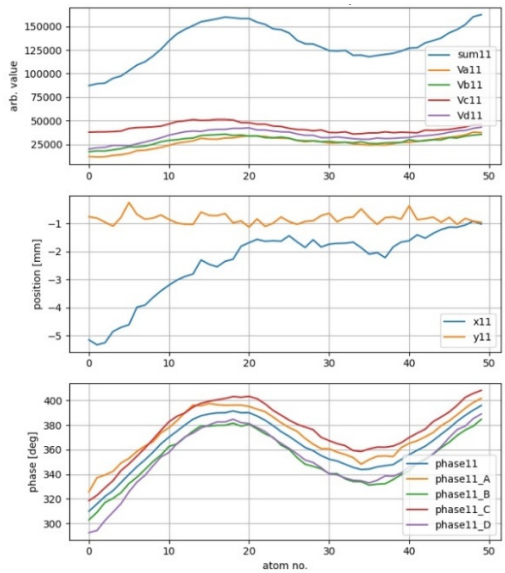

Figure 7: Position and phase measurement from LSPH. Upper: button signals and sum signal over 50 µs. Middle: position values. Lower: corresponding phase.

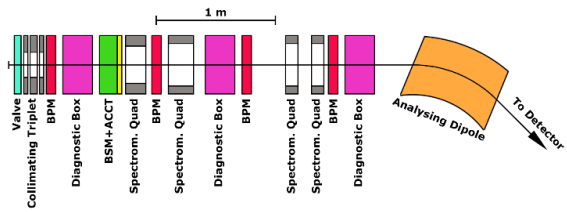

Figure 8: Schematic layout of the diagnostics testbench. The sketch is longitudinally at scale. ACCT: AC Current Transformer, BSM: Feschenko Bunch Shape Monitor.

A discussion of possible spectrometer designs can be found in [11]. The version currently under construction uses four already available quadrupoles and one of the two pLinac 45° dipoles, which create a point-to-point image of the spectrometer's input slit onto its output slit and generate the needed dispersive effect. It has a total length of ~6 m and extends ~1.7 m to the side. Simulations up to 5th order with the GICOSY [12] and MOCADI [13] codes show that the proton beam can be properly guided over the whole length of the testbench. While the first order estimate with a 250 µm slit resulted in a resolving power of ~4000, nonlinear effects reduce it to ~1000. Presently a mechanical design for the testbench has been worked out, and the field quality of the quadrupole magnets has been assessed.

ACKNOWLEDGEMENTS

The authors would like to thank the following people for their friendly and constructive support: Kajetan Fuchsberger, Matic Marn and Andrej Debenjak (COSYLAB), Dejan Tinta (ITECH), Kevin Lang, Wolfgang Kaufmann, Christoph Krüger, Sven Löchner, Peter Wieczorek, Michael Witthaus (GSI).

ISBN: 978-3-95450-215-8 ISSN: 2226-0366 doi:10.18429/JACoW-LINAC2022-TUPOJO06

REFERENCES

[1] O. K. Kester, "Status of the FAIR Facility", in *Proc. IPAC'13*, Shanghai, China, May 2013, paper TUXB101, pp. 1085-1089.

[2] M. Miski-Oglu et al., "Beam Commissioning of the Demonstrator Setup for the superconducting cw HMI/GSI Linac", 2019 J. Phys.: Conf. Ser. 1350 012089

[3] U. Ratzinger *et al.*, "A 70-MeV Proton Linac for the FAIR Facility Based on CH - Cavities", in *Proc. LINAC'06*, Knoxville, TN, USA, Aug. 2006, paper TH1004, pp. 526-530.

[4] M. Schütt, U. Ratzinger, and C. Zhang, "Development of a 325 MHz Ladder-RFQ of the 4-Rod-Type", in *Proc. IPAC'16*, Busan, Korea, May 2016, paper MOPOY024, pp. 899-901.

[5] G. Clemente et al., "Development of room temperature crossbar-H-mode cavities", Phys. Rev. ST Accel. Beams 14, 110101 (2011)

[6] T. Sieber *et al.*, "Beam Diagnostics Layout for the FAIR Proton Linac", in *Proc. LINAC'14*, Geneva, Switzerland, Aug.-Sep. 2014, paper THPP063, pp. 998-1000.

[7] Technical Design Report FAIR pLinac: https://edms.cern.ch/document/1332226/1

[8] M. Witthaus *et al.*, "SEM-GRID Prototype Electronics using Charge-Frequency-Converters", in *Proc. DIPAC'11*, Hamburg, Germany, May 2011, paper MOPD55, pp. 176-178.

[9] A. Navarro Fernandez, F. Roncarolo, and M. Sapinski, "Development of a Thermal Response Model for Wire Grid Profile Monitors and Benchmarking to CERN LINAC4 Experiments", in *Proc. IBIC'20*, Santos, Brazil, Sep. 2020, pp. 82-85. doi:10.18429/JACoW-IBIC2020-TUPP35

[10] P. Thieberger et al., "Fast readout algorithm for cylidrical beam position monitors providing good accuracy for particle bunches with large offsets", Review of Scientific Instruments 89, 043303 (2018)

[11] S. Udrea, P. Forck, C. M. Kleffner, K. Knie, and T. Sieber, "The Beam Diagnostics Test Bench for the Commissioning of the Proton Linac at FAIR", in *Proc. IBIC'19*, Malmö, Sweden, Sep. 2019, pp. 196-199. doi:10.18429/JACoW-IBIC2019-MOPP038

[12] https://webdocs.gsi.de/~weick/gicosy/

[13] https://webdocs.gsi.de/~weick/mocadi/